

Molecular Orientation and Mechanical Properties of Polymer Blends of PBT and a Liquid Crystalline Polyester

HYUK-SOO MOON,¹ JUNG-KI PARK,^{1,*} and JU-HWAN LIU²

¹Department of Chemical Engineering, Korea Advanced Institute of Science and Technology, 373-1, Kusung-dong, Yusung-gu, Daejeon, 305-701, South Korea; ²R & D Center, Petrochemicals & Polymers, Lucky Ltd., P. O. Box 10, Science Town, Daejeon, 305-343, South Korea

SYNOPSIS

A thermotropic liquid crystalline polyester (LCP) based on 4-hydroxyacetophenone azine and sebacoyl dichloride was synthesized via a low-temperature solution route. The liquid crystalline polymer was characterized by ¹H-NMR, DSC, GPC, and polarizing microscopy experiments. The LCP was melt-blended with poly(butylene terephthalate) (PBT), followed by the melt-spinning process at take-up speeds ranging from 14 to 50 m/min. We analyzed the molecular orientational order of LCP and PBT in as-spun fibers of the LCP/PBT blends by the attenuated total reflection (ATR) FTIR dichroism technique and WAXS. The order parameter (*S*), representing the molecular orientational order, of LCP in the polyblend fibers increased as the employed LCP amounts and the draw ratio increased. Moreover, the order parameter of PBT in the blends increased dramatically when sufficiently large amounts of LCP (over 50 wt %) were employed, especially for highly drawn fibers, which suggested a considerable miscibility between LCP and PBT. The thermal behavior of the blends investigated by DSC also indicated that the synthesized LCP was miscible, at least partially, with PBT. All these results correlated with the enhancement of mechanical properties observed for higher concentrations of LCP in the blends and for highly drawn samples. © 1996 John Wiley & Sons, Inc.

INTRODUCTION

It is well known that blends where liquid crystalline polymers (LCPs) reinforce thermoplastic polymers have potential use for high-strength, high-modulus, and lightweight materials. Their high modulus results from the molecular orientation of LCP in the nematic phase that can be aligned in the direction of flow with little shear or elongational strain.¹⁻⁵ LCP fibers exhibit a highly oriented structure even in the as-spun state, whereas conventional thermoplastic polymers do not. To obtain a molecular orientation, conventional thermoplastic polymers almost always need an additional stretching process.⁶⁻⁸

A number of studies have been reported for LCP blends with immiscible polymers.^{5-7,9-16} They indi-

cate that when the LCP is the minor phase the elongated LCP domains or fibrils with diameters of 1–10 μm are embedded in the matrix polymer, whereas a network structure forms at higher LCP contents. However, few studies dealing with LCP blends with partially miscible polymers not exhibiting fibrillar structure have been reported in the literature,^{2,17-20} and even fewer studies deal with the molecular orientation of such partially miscible LCP blend systems.^{19,20}

Characterization of molecular orientations in LCP blends is important since most of the physical and mechanical properties of the blends depend upon the extent of the LCP's orientation.^{19,21,22} Orientation of LCP can be measured by using a variety of techniques. Blackwall et al. showed that the X-ray diffraction data for the fibers drawn from the aromatic copolyesters based on *p*-hydroxybenzoic acid (HBA) and 2,6-hydroxynaphthoic acid (HNA) are consistent with a structure made up of oriented, extended chains of completely random monomer se-

* To whom correspondence should be addressed.

quence.^{23,24} Uzman et al. dealt with the orientational behavior of blends of polycarbonate (PC) or poly(methyl methacrylate) (PMMA) with a side-chain LCP during fiber drawing via optical and scanning electron microscopy (SEM), X-ray diffraction, and interfacial tension studies.²⁰ They indicated that, even in the fiber-drawing process, LCP droplets were not oriented in a PC matrix, but were oriented in a PMMA matrix. The different behavior between the two polymer blends were explained by the difference in the interfacial tension. Vibrational spectroscopy is particularly useful in the investigation of the molecular orientation since it is widely applicable, it often allows characterization of each component in the blends separately, and also it can be used to map orientation with high spatial resolution.^{21,22,25-34} For these reasons, FTIR attenuated total reflection (ATR) dichroism was chosen as an experimental technique in this study.

In this work, the molecular orientations of the component polymers in the polyblend fibers of PBT with a liquid crystalline polyester based on the mesogen 4-hydroxyacetophenone azine are analyzed as a function of composition and elongational shear, that is, draw ratio of as-spun fibers.

EXPERIMENTAL

Materials and Blends Preparation

An LCP with high molecular weight based on 4-hydroxyacetophenone azine and sebacoyl dichloride was prepared via a solution polycondensation at 0–60°C in a reactor equipped with a nitrogen inlet, a reflux condenser, an additional funnel, and a mechanical stirring assembly, which was a similar method to that used by Cimecioglu et al.³⁵⁻³⁸ The product was then characterized by nuclear magnetic resonance spectroscopy (¹H-NMR: Bruker-AM-300 NMR spectrometer [300 MHz]), differential scanning calorimetry (DSC: DuPont 9900 thermal analyzer), infrared spectroscopy (FTIR: Bio-Rad FTS 65 FTIR spectrometer), gel permeation chromatography (GPC: Waters CV-150 instrument equipped with three μ -Styragel columns [10^3 , 10^4 , and 10^5 Å]), and polarized optical microscopy (POM: Leitz LABORLUX 12POLIS instrument equipped with a 35 mm camera). Poly(butylene terephthalate) (PBT) was an injection grade supplied from the Cheil Synthetics.

The LCP powders and PBT pellets were combined in the ratios of 10/0, 8/2, 5/5, 2/8, and 0/10 to give mixtures of 3 g. The whole mixture was

tumbled together in a container and melt-extruded through a CSI mini mixing extruder (Model CS-194) at 225°C, which is above the melting temperature of PBT (220°C) and the solid–nematic transition temperature of the LCP (215°C). Before blending, the components were carefully dried in a dynamically evacuated oven at 100°C for at least 24 h to prevent any hydrolytic scission. The polyblend filaments were then spun into ambient air at 25°C and were taken up with a CSI take-up instrument (Model CS-194T). A 33 mm-diameter bobbin was used in the spinning of polyblend fibers of 50–300 μ m diameter, and the take-up speed was varied between 14 and 50 m/min.

Thermal Measurements

Thermal analyses of the blends were carried out under nitrogen atmosphere by DSC. A heating rate of 20°C/min was utilized, and the material was scanned from 30 to 300°C, from which the heating thermogram was obtained.

Mechanical Measurements

The mechanical properties of the drawn fibers, as a function of composition and draw ratio, were measured with an Instron universal testing machine at room temperature using a crosshead speed of 10 mm/min and a gauge length of 25 mm. All the properties reported are based on the initial cross-sectional area, and the results represent averages over at least five individual measurements.

Order Parameters Measurements

ATR spectra of the polyblend fibers were taken with a Digilab FTS-65 FTIR spectrometer, with typically 100 scans at a resolution of 4 cm^{-1} . Internal reflection elements of KRS-5, $10 \times 5 \times 1$ mm, were used with a variable-angle ATR accessory (TMP-V00 from Harrick). Polarization was accomplished with a wire grid polarizer which ensured 99.8% polarization. All the ATR spectra were obtained at an incidence angle of 45° (normal to the entrance aperture) and at room temperature. The dichroic ratio D was determined from the ratio of the absorbance A_{\parallel} and A_{\perp} measured with the IR radiation polarized parallel to and perpendicular to, respectively, the fiber drawing direction. Absorption values were assigned using peak height measurements and local base lines directly from the ATR spectra. Sample spectra were ratioed against background spectra

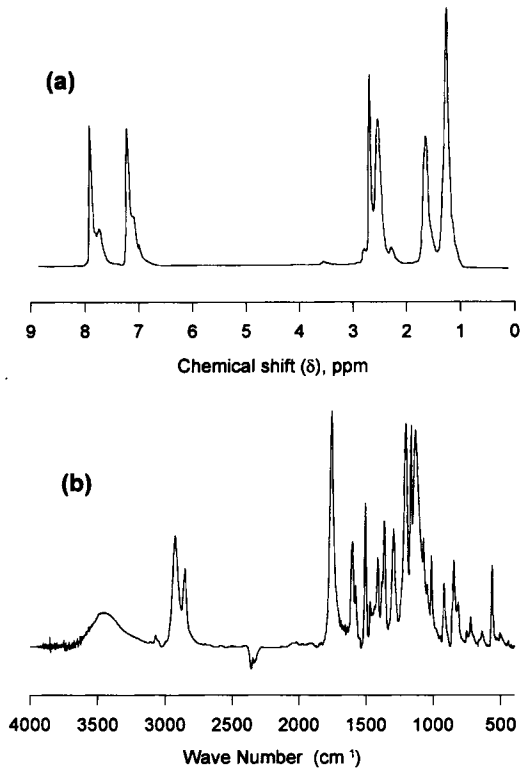


Figure 1 (a) $^1\text{H-NMR}$ and (b) FTIR spectra of the liquid crystalline polyester.

corresponding to each polarization and sample change.

WAXS Observation

Wide-angle X-ray diffraction patterns of the as-spun fibers were obtained using a flat plate-type camera and nickel-filtered $\text{CuK}\alpha$ radiation. These patterns were used to determine the qualitative features of the molecular orientation and to confirm the results from the ATR-IR experiment.

RESULTS AND DISCUSSION

Characterization of LCP

The structural evaluation of the LCP was made by $^1\text{H-NMR}$ and FTIR spectra given in Figure 1. $^1\text{H-NMR}$ and IR analysis results of the LCP are summarized below;

$^1\text{H-NMR}$: α -Methylene (2.58 ppm), β -methylene (1.77 ppm), other methylene (1.3–1.43 ppm), methyl (2.3 ppm), *para*-substi-

tuted phenyl (7.06–7.15, 7.92–7.94 ppm), end methoxy (3.6 ppm).^{35,36}

FTIR: Carbonyl $\text{C}=\text{O}$ stretching (1750 cm^{-1}), phenyl ring $\text{C}=\text{C}$ stretching ($1600, 1506\text{ cm}^{-1}$), $\text{C}-\text{H}$ deformation in *para*-substituted phenyl (814 cm^{-1}), symmetric antisymmetric $\text{C}-\text{O}-\text{C}$ stretching ($1150\text{--}1250\text{ cm}^{-1}$), CH_2 rocking vibration in methylene (844 cm^{-1}).^{36,39,40}

The number-average molecular weight of the LCP was determined by end-group analysis using $^1\text{H-NMR}$ spectroscopy. The aliphatic chain ends were assumed to be converted to the methyl ester, and these were titrated by measuring the peak intensity of $-\text{OCH}_3$ proton at $\delta = 3.6$ ppm as shown in Figure 1. Table I reveals the thermodynamic properties from DSC and average molecular weights measured by $^1\text{H-NMR}$ and GPC. The synthesized LCP was a relatively high molecular weight polymer ($\overline{M}_n \sim 84,300$) feasible for melt spinning and showed a nematic state at the processing window of PBT ($T_m = 220^\circ\text{C}$). The “polystyrene equivalent” molecular weight of the LCP from GPC was somewhat higher than the molecular weight from NMR, which was suspected due to the differences in the hydrodynamic volume of the LCP and polystyrene. Other details of the characterization of the LCP have been described previously.³⁵

Table I Thermal and Molecular Weight Analysis of the LCP

DSC	Heating	T_{K-N} ($^\circ\text{C}$)	213
		ΔH_{K-N} (J/g)	16.5
		T_{N-I} ($^\circ\text{C}$)	269
	Cooling	ΔH_{N-I} (J/g)	21.3
		T_{I-N} ($^\circ\text{C}$)	249
		ΔH_{I-N} (J/g)	10.5
GPC	T_{N-K} ($^\circ\text{C}$)	179	
	ΔH_{N-K} (J/g)	11.3	
	\overline{M}_n	84,300	
	\overline{M}_w	90,800	
NMR	Polydispersity	1.08	
	\overline{M}_n	64,500	

T_{K-N} : crystalline-nematic transition peak temperature; T_{N-I} : nematic-isotropic transition peak temperature; T_{I-N} : isotropic-nematic transition peak temperature; T_{N-K} : nematic-crystalline transition peak temperature; ΔH_{K-N} : enthalpy of crystalline-nematic transition; ΔH_{N-I} : enthalpy of nematic-isotropic transition; ΔH_{I-N} : enthalpy of isotropic-nematic transition; ΔH_{N-K} : enthalpy of nematic-crystalline transition.

Thermal Properties of LCP/PBT Blends

The thermal behavior of the LCP/PBT blends is tabulated and given in Table II. It also shows the thermal properties of pure LCP and PBT to provide a reference. The crystalline–nematic transition peak temperature (T_{K-N}) and the nematic–isotropic transition peak temperature (T_{N-I}) of the LCP phase in the LCP/PBT blends are about 212 and 269°C, respectively, which are nearly the same values as those of pure LCP. However, the enthalpy of the crystalline–nematic transition (ΔH_{K-N}) and the enthalpy of nematic–isotropic transition (ΔH_{N-I}) of the LCP phase in the blend decrease markedly from 16.5 and 21.3 J/g LCP for pure LCP to 3.1 and 9.5 J/g LCP for 50 wt % PBT blend, respectively.

The above thermodynamic phenomena of the drop in the enthalpies of transitions of the LCP due to the addition of PBT are attributable to the partial miscibility of the two components since PBT in the blends might act as an impurity to the LCP phase and reduce the stability of the nematic phase. Although the partial miscibility of components in polymer blends are characterized by the change of the glass transition temperature (T_g), in general, it was difficult to measure the change of the T_g in this work since the T_g 's of the PBT and LCP are quite similar, i.e., ca. 48 and 35°C for PBT and LCP, respectively, and the two polymers are semicrystalline polymers having crystalline fractions not showing a glass transition at all. An additional possibility for the description of the phenomena is that the blends may have undergone transesterification during the melt-extrusion process, since, in this study, the residence time in the extruder was about 10 min at 230°C. Though it is found in the literature that there is a certain induction period before the transesterification reaction can proceed to an appreciable extent and this induction period is again dependent on the temperature,^{2,17,18} it is proposable that transesterification reaction may occur during 10 min residence time in the extruder at 230°C in our blend system. Similarly, Sukhadia et al. reported that only 4.5–6 min of an induction period was necessary before the transesterification reaction between two copolyesters of poly(ethylene terephthalate) (PET) and *para*-hydroxybenzoic acid in 40/60 and 20/80 mol % could be observed based on DSC studies.¹⁷

Solvent-extraction results also indicate that some chemical reaction has occurred in the blends of the LCP and PBT during the extrusion process. After the Soxhlet extraction of the LCP/PBT blends with chloroform, which is a selective solvent for the LCP, the residue of the blends have exceeded the initial

Table II DSC Analysis of LCP/PBT Blends

	LCP/PBT				
	10/0	8/2	5/5	2/8	0/10
Heating					
T_{K-N} (°C)	213	212	212		
ΔH_{K-N} ^a	16.5	6.9	3.1		
T_m (°C)		223	227	226	226
ΔH_m ^b		64.5	55.5	44.7	46.7
T_{N-I} (°C)	269	267	268	269	
ΔH_{N-I} ^a	21.3	10.7	9.5	2.9	

T_m : peak temperature of melting endotherm of PBT phase; ΔH_m : heat of fusion of PBT phase. See footnote to Table I for additional abbreviations.

^a Enthalpy of transition recalculated per gram LCP.

^b Heat of fusion recalculated per gram PBT.

PBT contents in the blends. This result may suggest that some reaction such as a transesterification reaction has taken place between the LCP and PBT.

Measurements of Order Parameters Using ATR-IR Dichroism Technique

To understand the dependence of molecular orientation of the LCP and PBT in their blends upon mechanical fields and the presence of other component, ATR-IR dichroism measurements were made on the LCP/PBT blends with varying composition. The salient features of the polarized transmission FTIR spectra of LCP are illustrated in Figure 2. The two spectra obtained with the IR radiation polarized parallel and perpendicular, respectively, to the fiber direction vector seem to be quite different. Figure 2 shows that the 1500 and 1150–1250 cm^{-1} bands have parallel character, while the 1750, 844, and 560 cm^{-1} (O—C—O bending vibration) bands have perpendicular character.⁴¹

The average orientation of macromolecular chains relative to the fabrication extension direction can be expressed in terms of the order parameter as

$$S = \frac{1}{2} \langle 3 \cos^2 \theta - 1 \rangle \quad (1)$$

where θ is the angle between the chain axis of the molecule and the fiber direction vector and the angle brackets symbolizes an average of all the molecules. The order parameter can be related to the dichroic ratio obtained from infrared measurements of the principal adsorption coefficients for radiation parallel (A_{\parallel}) and perpendicular (A_{\perp}) to the extension direction ($D = A_{\parallel}/A_{\perp}$) by

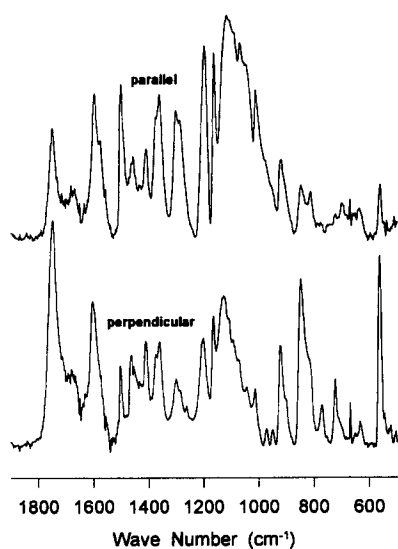


Figure 2 Polarized ATR-IR spectra of the LCP measured with E parallel and perpendicular to the fiber direction or draw axis.

$$S = \frac{(D - 1)(D_0 + 2)}{(D + 2)(D_0 - 1)} \quad (2)$$

where $D_0 = 2 \cot^2 \alpha$ and α is the angle between the chain axis and the transition moment. In our ATR-IR dichroism studies, the absorption bands at 844 and 1750 cm^{-1} were used to represent the orientation of LCP, assuming that the transition dipole mo-

ments are perpendicular to the long axis of the molecule.

The determination of S of PBT through ATR-IR dichroism measurements proceeds as follows: The absorption band at 1715 cm^{-1} for PBT, which did not overlap with any absorption bands of the LCP, was used in this study. With this band, which is assigned to the C=O stretching vibration mode with the dipolar transition moment perpendicular to the chain axis, the S values of PBT can be calculated according to eq. (2) in the same manner as for LCP.

The angle α for each absorption band is not known accurately. As a first approximation, we used 90° for all the perpendicular bands. If the angle is less than 90°, the order parameters calculated assuming 90° should be underestimated values and, therefore, minimum orientation values. Table III summarizes the dichroic ratios based on eqs. (1) and (2) of the LCP/PBT blends.

Figures 3 and 4 show the order parameters of LCP and PBT, respectively, in the LCP/PBT blends with various draw ratios. The S values were calculated with eq. (2) and the dichroic ratios at 1750 cm^{-1} band for the LCP phase and the dichroic ratios at 1715 cm^{-1} band for PBT. In addition, we could also estimate the order parameters of LCP for 844 cm^{-1} and the results are plotted in Figure 5. Since the draw ratio of as-spun fiber may be defined as [fiber diameter before spinning (d_0)/fiber diameter after

Table III Dichroic Ratios of LCP/PBT Blends

LCP/PBT	Diameter (μm)	844 cm^{-1}	1715 cm^{-1}	1750 cm^{-1}
10/0	63 \pm 7	0.202		0.341
	100 \pm 15	0.249		0.393
	149 \pm 33	0.324		0.512
8/2	77 \pm 23	0.309	0.673	0.44
	105 \pm 10	0.378	0.708	0.477
	108 \pm 24	0.403		0.489
	152 \pm 19	0.482	0.836	0.612
5/5	67 \pm 9	0.336	0.793	0.495
	90 \pm 9	0.386	0.822	0.581
	140 \pm 17	0.439	0.913	0.653
2/8	65 \pm 3		0.896	0.812
	69 \pm 12			0.808
	71 \pm 10	0.816	0.908	0.824
	128 \pm 18	0.899	0.941	0.915
0/10	70 \pm 15		0.906	
	72 \pm 9		0.9	
	98 \pm 13		0.921	
	255 \pm 37		0.949	

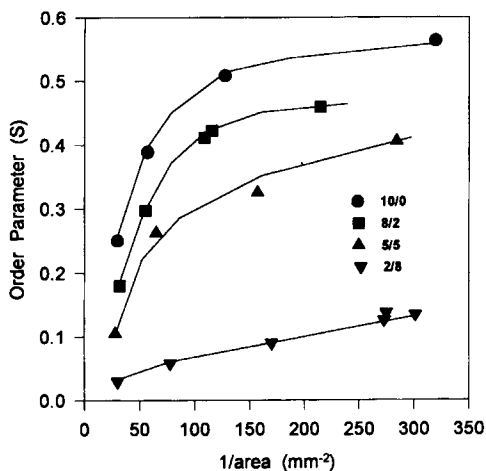


Figure 3 Order parameters of LCP phase in the LCP/PBT blends with respect to the draw ratio, monitored at 1750 cm^{-1} . The abscissa title $1/\text{area}$ represents a relative draw ratio.

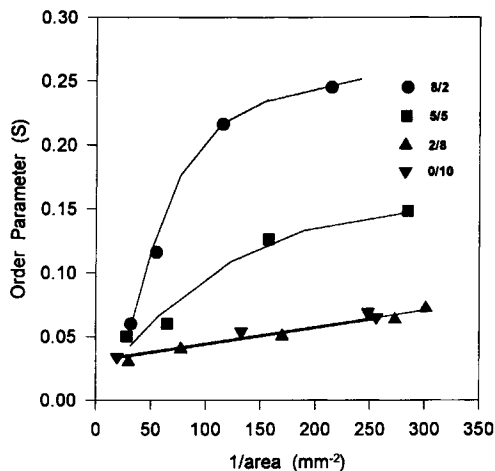


Figure 4 Order parameters of PBT phase in the LCP/PBT blends with respect to the draw ratio, monitored at 1715 cm^{-1} . The abscissa title $1/\text{area}$ represents a relative draw ratio.

spinning (d)]² in general, under the assumption of constant volume of fiber,^{8,42-44} and since d_0 is a constant, though we do not know the exact value, the abscissa title $1/\text{area}$ in Figures 3-5 is a parameter corresponding to a relative draw ratio.

In Figure 3, one can see that the S values of the LCP phase in LCP/PBT = 10/0, 8/2, and 5/5 blends, where LCP contents are above 50 wt %, are around 0.5, which is a substantially high value. One can also find that the rate of increase in the LCPs order parameters due to drawing decreases sharply when $1/\text{area}$ is around 100. The saturating tendency of S with increasing the draw ratio is also observable for the PBT phase in LCP-rich blends as shown in Figure 4. However, the order parameters of both LCP and PBT in the LCP/PBT = 2/8 blend, which may be morphologically different from LCP-rich blends, increase linearly as the draw ratio increases. It is to be noted that the dependence of S for the PBT phase in the LCP/PBT = 2/8 blend upon the draw ratio is almost the same as that of pure PBT, which suggests that the molecular orientation of PBT is not affected by the presence of LCP when PBT forms a matrix.

All the above results are somewhat predictable, since the two-component polymers used in our blend system seem to be partially miscible in the previous DSC studies and the melt-blending process was taken above 230°C , which is a sufficiently high temperature to initiate the transesterification reaction between LCP and PBT. The transesterification reaction may bring two components close enough to make one component affect significantly the other's

molecular motion. It is suggested that PBT leads the molecular motions of LCP in PBT-rich blends under elongational field, whereas the molecular motions of PBT follow those of LCP when LCP is the major component. Consequently, the order parameters of PBT, which relaxes fast and has poor orderability, in LCP-rich blends are enhanced significantly compared with the order parameters of pure PBT as shown in Figure 4.

The change pattern of the order parameter as a function of draw ratio for the LCP bands at 1750 and 844 cm^{-1} , as presented in Figures 3 and 5, respectively, is quite similar, but the value of the order

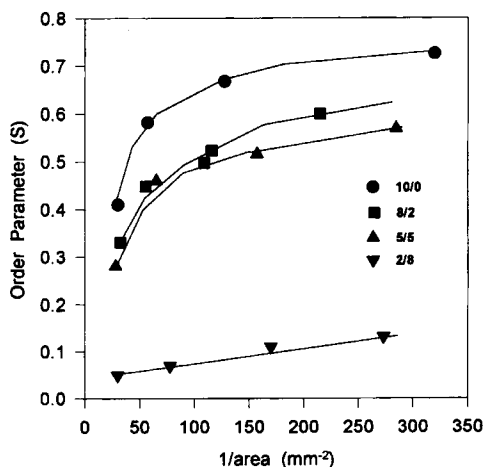


Figure 5 Order parameters of LCP phase in the LCP/PBT blends with respect to the draw ratio, monitored at 844 cm^{-1} . The abscissa title $1/\text{area}$ represents a relative draw ratio.

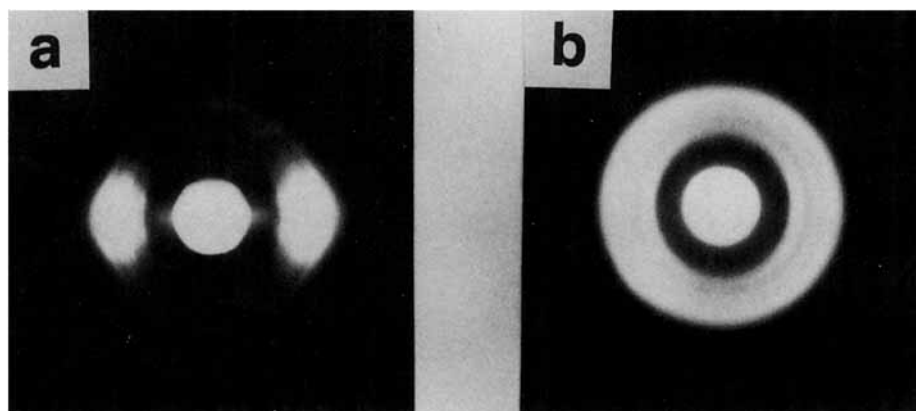


Figure 6 WAXS patterns of (a) LCP and (b) PBT fibers of ca. $100 \pm 10 \mu\text{m}$ diameter. Extrusion temperature = 230°C . Air-quenched.

parameter differs in magnitude for the different bands. This deviation suggests that the assumption of a right angle between the transition moment vector for the vibrations and the chain axis is not strictly correct. However, since we are interested in the relative orientations for a given band, it is not necessary to make any corrections in this regard.

Even though we neglected the difference in magnitude between Figures 3 and 5, there is another interesting difference between the two figures. The order parameters of the LCP phase for the LCP/PBT = 8/2 blend are considerably larger than those for the LCP/PBT = 5/5 blend when the order parameters of the LCP phase are obtained from the ester C=O stretching band at 1750 cm^{-1} , whereas the order parameters of the LCP phase from the methylene band at 844 cm^{-1} are similar for the two blends. Since the methylene region of LCP is less disturbed by the molecular interaction with PBT than is the ester region, the more realistic molecular orientations of the LCP may be represented by the order parameters from the methylene region. Therefore, it is suggested from Figure 5 that the molecular orientation of the LCP does not decrease in proportion to the amounts of the employed PBT. The molecular orientations of LCP in the blend with PBT was reduced a little by the environmental PBT molecules but the degree of reduction was not significant when LCP contents were more than 50 wt %. However, the LCP's molecular orientations were completely dependent upon PBT when LCP contents were less than 20 wt % and, subsequently, LCP molecules were sufficiently dispersed over the PBT phase.

The considerable difference in the order parameters of LCP phase for the LCP/PBT = 5/5 and LCP/PBT = 8/2 blends as shown in Figure 3 can

be explained as follows: The more PBT employed in the blends, the more PBT molecules lie around the LCP molecule and the greater is the probability of the transesterification reaction to occur. Furthermore, the two ester-based polymers may interact principally at their ester linkages. The transesterification and/or mutual interaction between LCP and PBT are believed to interrupt the transition moment of C=O stretching vibration of LCP, and, consequently, the order parameters of the LCP phase obtained from the ester band for the LCP/PBT = 5/5 blend are apparently less than those for the LCP/PBT = 8/2 blend (Fig. 3), even though the molecular orientations of LCP in the LCP/PBT = 5/5 blend are comparable to the molecular orientations in the LCP/PBT = 8/2 blend (Fig. 5).

Qualitative Measurements of Molecular Orientation Using WAXS Technique

Figure 6 shows WAXS patterns of pure LCP and pure PBT fibers spun with the same draw ratio to have diameters of ca. $100 \pm 10 \mu\text{m}$. The drawing direction corresponded to the vertical direction in the diagram. The scattering diagram of the pure PBT shows no intensity maxima in the equatorial or meridional regions, which suggests that the PBT has no preferred orientation despite the melt-spinning process. However, the scattering of the LCP fibers shows a distinct concentration of intensity around the equator, suggesting well-developed orientations of the molecular chains parallel to the drawing direction. All these results coincide with the ATR-IR studies which indicate the order parameter of PBT of ca. $98 \pm 10 \mu\text{m}$ diameter as 0.04 and that of LCP of ca. $100 \pm 17 \mu\text{m}$ as 0.66.

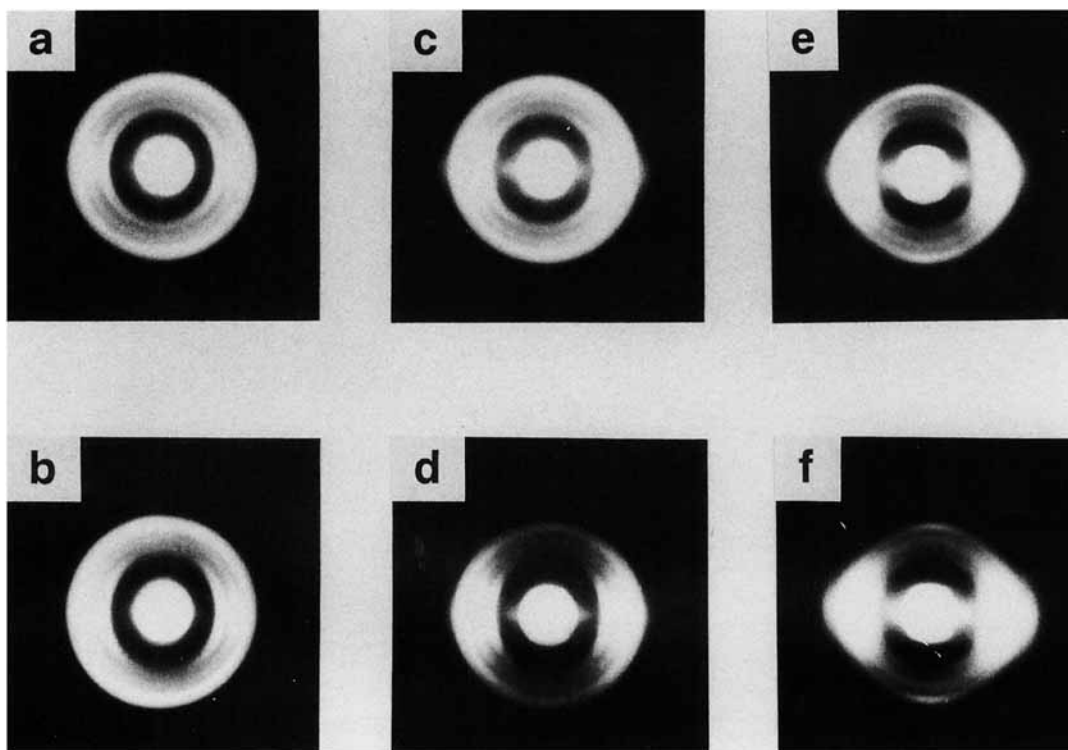


Figure 7 Effect of blend composition and draw ratio on WAXS patterns of the LCP/PBT blend fibers. Extrusion temperature = 230°C. LCP/PBT = 2/8: (a) $132 \pm 18 \mu\text{m}$; (b) $67 \pm 8 \mu\text{m}$. LCP/PBT = 5/5: (c) $140 \pm 17 \mu\text{m}$; (d) $90 \pm 9 \mu\text{m}$. LCP/PBT = 8/2: (e) $152 \pm 19 \mu\text{m}$; (f) $98 \pm 14 \mu\text{m}$.

The molecular orientation of LCP and PBT in their blends as a function of composition and draw ratio was also investigated via a scattering technique. The WAXS patterns of the low-drawn (diameters of ca. $140 \pm 15 \mu\text{m}$) and high-drawn (diameters of ca. $80 \pm 10 \mu\text{m}$) LCP/PBT polyblend fibers are shown in Figure 7. All diagrams confirm the phenomena revealed in the previous ATR-IR studies that the higher content of LCP and the higher drawing cause the higher molecular orientations of LCP as well as PBT in the LCP/PBT blends. Hence, we can expect that the molecular orientations of surface and bulk show qualitatively similar dependence upon the blend composition and draw ratio, and, therefore, the order parameters obtained from ATR-IR dichroism studies can represent bulk molecular orientational order as well as surface in spite of that the ATR measurements are sensitive only to a depth of about $5 \mu\text{m}$ into the surface of the fiber as an instrumental limitation.^{27,33}

Measurements of Mechanical Properties

The results obtained for the tensile modulus of the LCP/PBT blends melt-spun with various take-up

speeds are presented in Figure 8. For all the blends, the tensile modulus is enhanced as the fiber diameter decreases or the draw ratio increases. Moreover, it is possible to classify the blends into two according to the increase of their tensile modulus with the draw

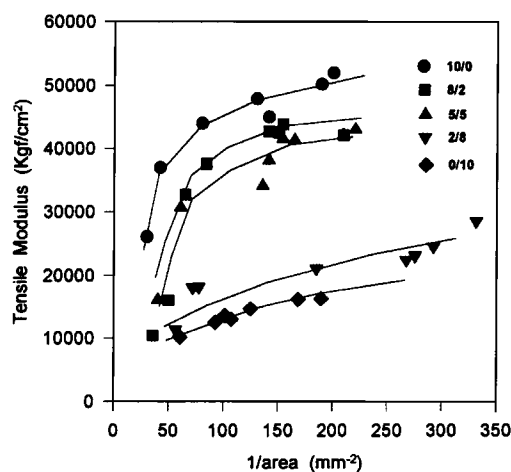


Figure 8 Tensile modulus vs. draw ratio of LCP/PBT blends. The abscissa title $1/\text{area}$ represents a relative draw ratio.

ratio. For the LCP/PBT = 10/0, 8/2, and 5/5 blends which contain relatively large amounts of LCP, the tensile modulus enhances drastically as the draw ratio increases up to the abscissa parameter 1/area in Figure 8 of about 100, and then the additional drawing contributes little to the enhancement of tensile modulus, whereas a constant increase in the modulus as a function of draw ratio is observed for the PBT-rich blends, i.e., LCP/PBT = 2/8 and 0/10 blends.

It is interesting to note that the characteristics of the tensile modulus as a function of blend composition and draw ratio (Fig. 8) correspond well with those of order parameters of the LCP phase in the LCP/PBT blends as a similar function (Fig. 5). These observations indicate that the major contribution to the tensile modulus comes from the molecular orientation of the LCP phase, which is a similar conclusion with that of previous studies by Ajji et al.¹⁹

CONCLUSION

It has been demonstrated, in this study, that when the blends of LCP with PBT are melt-spun with various draw ratios, the molecular orientations of LCP in the blends are interrupted by the PBT and the order parameter of LCP phase decreases as the contents of PBT increase, whereas the molecular orientations of PBT are enhanced by the LCP and the order parameter of PBT phase exceeds that of pure PBT and increases for the blends richer in LCP. For all the blends, the molecular orientations of the components are improved as the draw ratio increases up to 1/area, which is a parameter representing the relative draw ratio, of about 100, and further drawing does not affect significantly the molecular orientation of the component polymers.

The investigation of mechanical properties indicates that the addition of up to 20 wt % of LCP upon PBT does not improve markedly the tensile modulus of the blends. However, a dramatic enhancement of tensile modulus is obtained when sufficiently large amounts of LCP (over 50 wt %) are employed, especially for highly drawn polyblend fibers. It is proposed that the molecular orientational behavior of the LCP phase would be responsible for the increase in the mechanical properties observed for the blends.

The authors gratefully acknowledge the financial support on this work from the Ministry of Science and Technology.

REFERENCES

1. C. S. Brown and P. T. Alder, in *Polymer Blends and Alloys*, M. J. Folkes, and P. S. Hope, Eds., Chapman & Hall, London, UK, 1993.
2. G. V. Laivins, *Macromolecules*, **22**, 3974 (1989).
3. J. I. Kroschwitz, *High Performance Polymers and Composites*, Wiley, New York, 1991.
4. D. Dutta, H. Fruitwala, A. Kohli, and R. A. Weiss, *Polym. Eng. Sci.*, **30**, 1005 (1990).
5. G. Kiss, *Polym. Eng. Sci.*, **27**, 410 (1987).
6. Y. Qin, D. L. Brydon, R. R. Mather, and R. H. Wardman, *Polymer*, **34**, 1196 (1993).
7. Y. Qin, D. L. Brydon, R. R. Mather, and R. H. Wardman, *Polymer*, **34**, 1202 (1993).
8. H. P. Nadella, H. M. Henson, J. E. Spruiell, and J. L. White, *J. Appl. Polym. Sci.*, **21**, 3003 (1977).
9. W. C. Lee and A. T. Divenedetto, *Polym. Eng. Sci.*, **32**, 400 (1992).
10. G. Crevecoeur and G. Groeninckx, *Polym. Eng. Sci.*, **30**, 532 (1990).
11. M. T. Heino and J. V. Sepala, *J. Appl. Polym. Sci.*, **44**, 2185 (1992).
12. M. T. Heino and J. V. Sepala, *J. Appl. Polym. Sci.*, **48**, 1677 (1993).
13. K. G. Blizard, C. Federici, O. Federico, and L. L. Chappoy, *Polym. Eng. Sci.*, **30**, 1442 (1990).
14. F. P. La Mantia, A. Valenza, M. Paci, and P. L. Magagnini, *Polym. Eng. Sci.*, **30**, 7 (1990).
15. D. Beery, S. Kenig, A. Siegmann, and M. Narkis, *Polym. Eng. Sci.*, **32**, 14 (1992).
16. R. A. Weiss, W. Huh, and L. Nicolais, *Polym. Eng. Sci.*, **27**, 684 (1987).
17. A. M. Sukhadia, D. Done, and D. G. Baird, *Polym. Eng. Sci.*, **30**, 519 (1990).
18. J. F. Croteau and G. V. Laivins, *J. Appl. Polym. Sci.*, **39**, 2377 (1990).
19. A. Ajji, J. Brisson, and Y. Qu, *J. Polym. Sci. Polym. Phys. Ed.*, **30**, 505 (1989).
20. M. Uzman, K. Kuhupast, and J. Springer, *Makromol. Chem.*, **190**, 3185 (1989).
21. J. M. Chalmers and N. J. Everall, in *Polymer Characterisation*, B. J. Hunt and M. I. James, Eds., Chapman & Hall, London, UK, 1993.
22. A. Pirnia and C. S. P. Sung, *Macromolecules*, **21**, 2699 (1988).
23. J. Blackwell, G. A. Gutierrez, and R. A. Chivers, *Macromolecules*, **17**, 1219 (1984).
24. J. Blackwell, G. A. Gutierrez, R. A. Chivers, and W. J. Ruland, *J. Polym. Sci. Polym. Phys. Ed.*, **22**, 1343 (1984).
25. F. M. Mirabella, Jr., M. J. Shankernarayanan, and P. L. Fernando, *J. Appl. Polym. Sci.*, **37**, 851 (1989).
26. M. Theodorou and B. Jasse, *J. Polym. Sci. Polym. Phys. Ed.*, **24**, 2643 (1986).
27. F. M. Mirabella, Jr., *J. Polym. Sci. Polym. Phys. Ed.*, **21**, 2403 (1983).
28. C. S. P. Sung, *Macromolecules*, **14**, 591 (1981).

29. A. Lee and R. P. Wool, *Macromolecules*, **19**, 1063 (1986).
30. F. M. Mirabella, Jr., *J. Polym. Sci. Polym. Phys. Ed.*, **25**, 591 (1987).
31. Y. Zhao, C. G. Bazuin, and R. E. Prud'homme, *Macromolecules*, **22**, 3788 (1989).
32. M. L. Sartirana, E. Marsano, E. Bianchi, and A. Ci-ferri, *Macromolecules*, **19**, 1176 (1986).
33. J. P. Hobbs, C. S. P. Sung, K. Krishnan, and S. Hill, *Macromolecules*, **16**, 193 (1983).
34. J. C. Lim, J. K. Park, and H. Y. Song, *J. Polym. Sci. Polym. Phys. Ed.*, **32**, 29 (1994).
35. D. W. Kim, J. K. Park, and K. S. Hong, in *Ordering in Macromolecular Systems*, A. Teramoto, M. Kobayashi, and T. Norisuje, Eds., Springer-Verlag, Berlin, Heidelberg, 1994.
36. A. L. Cimecioglu, H. Fruitwala, and R. A. Weiss, *Makromol. Chem.*, **191**, 2329 (1990).
37. A. Roviello and A. Sirigu, *Eur. Polym. J.*, **15**, 61 (1979).
38. P. Iannelli, A. Roviello, and A. Sirigu, *Eur. Polym. J.*, **18**, 745 (1982).
39. J. B. Lambert, D. A. Lightner, H. F. Shurvell, and R. G. Cooks, Eds., *Introduction to Organic Spectroscopy*, Macmillan, New York, 1987.
40. Z. Jedlinski, J. Franek, A. Kulczycki, A. Sirigu, and C. Carfagna, *Macromolecules*, **22**, 1600 (1989).
41. J. L. Koenig, *Spectroscopy of Polymers*, American Chemical Society, Washington, DC, 1992.
42. G. Y. Chen, J. A. Cuculo, and P. A. Tucker, *J. Appl. Polym. Sci.*, **44**, 447 (1992).
43. K. Itoyama, *J. Polym. Sci. Polym. Phys. Ed.*, **26**, 1845 (1988).
44. G. Y. Chen, J. A. Cuculo, and P. A. Tucker, *J. Polym. Sci. Polym. Phys. Ed.*, **26**, 1677 (1988).

Received December 29, 1994

Accepted July 2, 1995